Clinical Radiology 74 (2019) 805–812

Contents lists available at ScienceDirect

Clinical Radiology

journal homepage: www.clinicalradiologyonline.net

Effect of a saline flush technique for head and neck imaging in dual-energy CT: improvement of image quality and perivenous artefact reduction using virtual monochromatic imaging

H. Washio [a], S. Ohira [a,b,*], N. Kanayama [a], K. Wada [a], T. Karino [a], R. Komiyama [a], M. Miyazaki [a], T. Teshima [a]

[a] Department of Radiation Oncology, Osaka International Cancer Institute, Osaka, Japan
[b] Department of Medical Physics and Engineering, Osaka University Graduate School of Medicine, Suita, Japan

ARTICLE INFORMATION

Article history:
Received 17 April 2019
Accepted 12 June 2019

AIM: To evaluate the effect of the saline flush (SF) technique on the depiction of lesions and the reduction of perivenous artefacts in the head and neck region using dual-energy computed tomography (CT) with virtual monochromatic imaging (VMI).

MATERIALS AND METHODS: Fifty patients with head and neck cancer were divided into two groups: group A, without a SF and group B, with a 30-ml SF. All images were acquired using fast kilovolt-switching CT (Revolution HD, GE Healthcare, Milwaukee, WI, USA). Contrast-to-noise ratios (CNRs) of the lesions were calculated at VMI energy levels ranging from 40 to 80 keV. Subjective analysis of overall image quality, delineation of lesions, and perivenous artefacts was conducted by two reviewers at both VMI energy level 40 keV and the optimal energy level (which showed optimal CNR by objective analysis).

RESULTS: Optimal energy level was 63 keV for group A and 61 keV for group B. At VMI energy levels ranging from 40 to 80 keV, the CNR was higher for group B. The highest subjective overall image quality was shown for group B at the optimal energy level (subjective image quality mean value, 3.40). Subjective delineation of lesions was comparable. The perivenous artefact score was significantly higher for group B (2.44 versus 2.74 [$p<0.05$] at 40 keV, 3.20 versus 3.46 [$p<0.05$] at the optimal energy level).

CONCLUSION: The SF technique results in an improvement of lesion CNR and a reduction of perivenous artefacts in VMI using duel-energy CT, especially at 40 keV.

Introduction

Contrast-enhanced computed tomography (CT) is a valid imaging technique for tumour detection, radiation therapy treatment planning, and surgical guidance because of its high-speed acquisition, wide availability, relatively low costs, and high tumour enhancement.[1–3] Although artefacts

* Guarantor and correspondent: S. Ohira, Osaka International Cancer Institute, 3-1-69 Otemae, Chuo-ku, Osaka, 541-8567, Japan. Tel.: +81-6-6945-1181; fax: +81-6-6945-1900.
E-mail address: ueyama-si@mc.pref.osaka.jp (S. Ohira).

https://doi.org/10.1016/j.crad.2019.06.010
0009-9260/

caused from contrast materials remaining in the subclavian vein often disturb depiction of the perivenous region in contrast-enhanced CT examinations, many published studies have reported alleviation of this problem by injection of saline immediately after the inflow of contrast material. This saline flush technique enables not only perivenous artefact reduction, but also results in an improvement in vascular and tumour enhancement and reduction of the contrast material dose, by efficient use of contrast material existing in the injector tube and infused vein[3–10].

Dual energy computed tomography (DECT) is a state-of-the-art technique, which can now be used routinely in clinical imaging. This technique results in the acquisition of two image datasets from the same anatomical location with two different X-ray spectra. The resulting virtual monochromatic image (VMI) is depicted as if it had been imaged with a monochromatic beam at the given energy level (in kilo-electronvolts), as each type of material demonstrates a relatively specific pattern of attenuation changes between images obtained with high and low-energy spectra.[11] Recent studies have investigated the potential of VMI, acquired using DECT, compared to conventional imaging.[2,12–15] For example, metal artefact reduction with higher energy VMI,[12] and better delineation of tumours, with respect to adjacent to soft tissues, with lower energy VMI[2] have been reported. Lam *et al.*[13] demonstrated that in standard neck image reconstruction, the optimal signal-to-noise ratio (SNR) was at 65 keV and greatest tumour conspicuity was at 40 keV.

Tumour, lymph node, or vessel attenuations increase with lower energy VMIs because these energies approach the iodine *k* edge of 33.17 keV[13]; however, perivenous artefacts caused from contrast material remaining in the subclavian vein may also be more conspicuous at lower energy levels than conventional imaging. There are no studies that have determined whether the saline flush technique reduces perivenous artefacts and improves tumour, lymph node, or vessel depiction on the VMI.

The aim of the present study was to evaluate the effect of the saline flush technique on the depiction of tumours and metastatic lymph nodes and on the reduction of perivenous artefacts for VMI using DECT in the head and neck region.

Materials and methods

Patients

An ethics committee approved this study and written informed consent was obtained from each patient. A total of 50 patients, who had undergone DECT for radiation therapy planning between July 2017 and November 2018, were evaluated retrospectively. All patients had head and neck squamous cell carcinoma (SCC), confirmed by histopathological examination.

Patients were divided into two groups with different protocols (Table 1); group A, composed of 25 patients who were examined between July 2017 and May 2018 without using a saline flush after injection of contrast materials and group B, composed of 25 patients who were examined between June 2018 and November 2018 with a saline flush after injection of contrast materials.

Table 1
Patient characteristics and relevant *p*-values of the two patient groups: those with and without the saline flush technique in virtual monochromatic imaging using dual-energy computed tomography.

Clinical data	Group A (w/o SF)	Group B (w SF)	*p*-Value
Number of patients	25	25	
Age (years)			0.79
Median	65	66	
Range	28–81	32–90	
Sex (male/female)	21/4	20/5	0.71
Height (cm)			0.85
Mean	165.8±8.2	165.5±6.9	
Range	147–181	155–180	
Weight (kg)			0.90
Mean	60.4±12.5	60.8±10.2	
Range	40–92	44–88	
Body mass index (kg/m^2)			0.82
Mean	21.9±3.7	22.1±2.8	
Range	15–28	16–28	
Tumour site			
Nasopharynx	6	7	
Oropharynx	5	2	
Hypopharynx	10	10	
Supraglottis	4	6	
Number of evaluated metastatic LN[a]	15	15	
Saline flush (ml)	0	30	
Injection arm (right/left)	23/2	20/5	0.22

w/o SF, without the saline flush technique; w SF, with the saline flush technique; LN, lymph node.
[a] If there were several lymph nodes for one patient, we evaluated only the largest lymph node.

Image acquisition

All DECT examinations were performed on a fast kilovolt-switching CT system (Revolution HD, GE Healthcare, Milwaukee, WI, USA), switching tube voltages between 80 and 140 kV peak in <0.5 ms. The scanning parameters for patients of <66 kg were as follows: gemstone spectral imaging preset, number 22; 375 mA tube current, 0.7 seconds rotation time, 40 mm collimation width, 0.984 helical pitch, 512×512 matrix size, 2.5 mm section thickness, 15.02 mGy CT dose index volume. Patients who were >66 kg were scanned using the following parameters: gemstone spectral imaging preset, number 1; 630 mA tube current, 0.5 seconds rotation time, 40 mm collimation width, 17.77 mGy CT dose index volume. The automatic exposure control was not activated. All patients were injected with 450 mg iodine/kg contrast material (240 mg iodine/ml; Optiray, Fuji pharma, Tokyo, Japan or iopamidol 300, 370 mg iodine/ml; Bracco, Milano, Italy) with a fixed injection time (50 seconds). The flow rate was adjusted to body weight and injected contrast material density (1.5–1.9 seconds). In group B, 30 ml saline was immediately injected, with the same injection rate of the contrast material, after the injection of the contrast material. CT was performed with a scan delay of 70 seconds for group A and 80 seconds for group B. The delay of 10

seconds for group B compared to group A is due to the effect of prolongation of time to peak enhancement by following with the saline flush.[16] The acquired data were reconstructed with Adaptive Statistical Iterative Reconstruction (ASiR), blending level 30%.

Objective image analysis

All image series were transferred to an Advantage workstation version 4.7 (GE Healthcare) to perform objective image spectral analysis. For each patient, a circular regions of interest (ROI) was placed on an axial section in the tumour and metastatic lymph node, avoiding areas of necrosis, visible artefacts, sternocleidomastoid muscle (at the level of the vocal cord), and parotid gland to measure attenuation in mean Hounsfield units and standard deviation (SD). The SD in the sternocleidomastoid muscle was recorded as image noise. For each structure, three non-overlapping ROIs were placed. The measurements were also performed on the vascular system with ROIs placed in the following structures: common carotid artery (injection side and opposite side, at the level where near the division in internal and external carotid artery), internal jugular vein (injection side and opposite side, at the same level as that of common carotid artery), subclavian vein (injection side and opposite side, at the costoclavicular space between the first rib and the clavicle), and superior vena cava (at the level where the right pulmonary artery passes posteriorly).

The contrast-to-noise ratio (CNR) was calculated by using the formula:

CNR=(mean lesion enhancement−mean muscle attenuation)/SD measured in muscle,

In accordance with a previous study.[1] The CNR analysis was performed on the tumour and metastatic lymph node at different VMI energy levels ranging from 40 to 80 keV in 1 keV increments. Energy levels >80 keV were not reconstructed because iodine signal and tumour enhancement can be expected to reduce.[11] The CNR and the mean attenuation were compared between groups A and B at 40 keV (as this demonstrated greatest tumour conspicuity in a previous study[13]) and the optimal energy level, which showed the optimal CNR by objective analysis.

Subjective image analysis

Two radiologists (with 10 years and 6 years experience in radiation therapy, respectively) who were not involved in the design of the study were blinded to the energy setting of the VMI, evaluation of the other reviewer, and whether the saline flush technique was applied; however, they were aware that all the patients included in the study had been diagnosed with head and neck cancer. Images were arranged automatically in the standard window setting (level, 100 HU; width, 350 HU); however, reviewers were allowed to freely adjust these values to improve tumour visualisation while evaluating images. Subjective image quality of each image series was rated using a five-point scale for overall image quality (1=non-diagnostic, 2=poor, 3=moderate, 4=good, 5=excellent); delineation of lesion (1=no visual delineation to 5=excellent delineation), and perivenous artefacts (1=pronounced artefacts with blurred vessel edges to 5=no artefacts with sharp vessel edges).

Statistical analysis

Objective results are reported as mean±SD. Comparison of patient characteristics (age, height, weight, and body mass index) and objective image analysis between the two groups was undertaken by utilising the Mann−Whitney *U*-test. The ratios of sex and injection arm side (right or left arm) were analysed using the chi-squared test. Statistical analysis of subjective image quality was performed by averaging the reviewer's five-point score and using the Mann−Whitney *U*-test. The inter-rater agreement was calculated by using weighted kappa (*k*).[17] The *k* value was interpreted as follows: $k<0.2$, slight agreement; $k=0.21–0.40$, fair agreement; $k=0.41–0.60$, moderate agreement; $k=0.61–0.8$, substantial agreement; $k=0.81–1.0$, almost perfect agreement. The remaining statistical analysis was performed using SPSS Version 24 (IBM Corp, Armonk, NY, USA). A *p*-value of <0.05 was taken to indicate statistical significance.

Results

Objective image analysis

Fig 1 shows the CNR of the tumour and metastatic lymph node for groups A and B. Both CNR curves showed peak CNR at VMI of 63 keV (6.6±2.9 for tumour, 6±4 for metastatic lymph node) and 61 keV (9±3.1 for tumour, 8.1±3.8 for metastatic lymph node) for group A and B, respectively. As the VMI energy level increases, the CNR gradually declined after reaching peak energy. The peak energy level was utilised in subsequent data analysis as the "optimal energy". The greatest difference in the mean CNR between group A and B was observed at 40 keV (2.7 for tumour, 2.9 for metastatic lymph node).

The mean values and *p*-values of objective analyses are shown in Table 2. Tumour enhancement was significantly higher for group B than for group A (group A versus B, 193.5±31.1 versus 221.1±32.8 HU [$p<0.01$] at 40 keV, 98.4±13.9 versus 113.7±15.2 HU [$p<0.01$] at the optimal energy). There were no significant differences in the mean metastatic lymph node enhancement (40 keV, optimal energy; $p=0.12$, $p=0.08$), sternocleidomastoid muscle ($p=0.52$, $p=0.09$), parotid gland attenuation ($p=0.71$, $p=0.79$) and noise ($p=0.22$, $p=0.71$) between groups A and B. The tumour and metastatic CNR were significantly higher for group B than A (group A versus B, 6.3±2.3 versus 9±3.1 [$p<0.01$] for the tumour at 40 keV, 6.6±2.9 versus 9±3.1 [$p<0.01$] for the tumour at optimal energy, 5.8±3.0 versus 8.7±3.8 [$p<0.05$] for the lymph node at 40 keV), although a significant difference was not found for metastatic lymph nodes at the optimal energy (6±4.0 versus 8.1±3.8 [$p=0.25$]).

There was no significant difference between both groups for mean common carotid artery attenuation ($p=0.68$ for

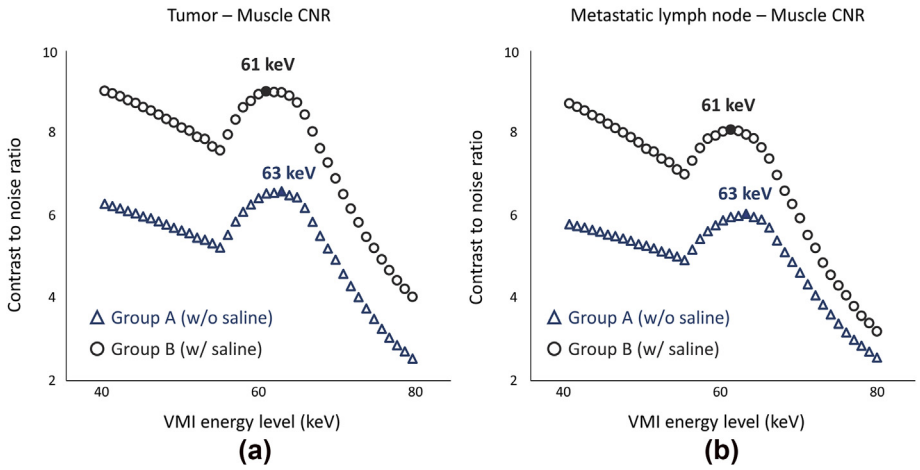

Figure 1 CNR analysis at different VMI energy levels. CNR analysis for (a) tumour and (b) metastatic lymph node at different VMI energy levels ranging 40–80 keV in 1 keV increments. The optimal CNR were observed at 61 keV for group A (without the saline flush technique) and at 63 keV for group B (with the saline flush technique).

injection side at 40 keV, p=0.46 at optimal energy, p=0.68 for opposite side at 40 keV, p=0.13 at optimal energy). Injection side internal jugular vein, subclavian vein, and superior vena cava attenuation for group A was significantly higher than that of group B at 40 keV (group A versus B, 517.3±89.7 versus 461±59.9 HU [p<0.01] for the internal jugular vein, 825.9±642.0 versus 466±152.7 HU [p<0.01] for the subclavian vein and 439.4±137.2 versus 415.2±56.7 HU [p<0.05] for the superior vena cava).

Subjective image analysis

The mean values, k coefficients, and p-values of image quality scores from both reviewers are summarised in Table 3. Examples of the image impression for both groups with different energy settings are given in Figs 2–4. The mean rating of overall image quality was significantly higher for group B than group A at the optimal energy (group A versus B, 3.16 versus 3.40 [p<0.05]), but a significant difference was not found at 40 keV VMI (2.70 versus 2.72 [p=0.78]); however, the mean score for delineation of lesions was comparable at 40 keV VMI (3.04 versus 3.02 [p=0.78]). At optimal energy VMI, the value was higher for group B with no significant difference (2.88 versus 3 [p=0.59]). The subjective quality score regarding perivenous artefacts was significantly higher for group B than A at both energy levels (2.44 versus 2.74 [p<0.05] at 40 keV, 3.20 versus 3.46 [p<0.05] at optimal energy).

Discussion

In the present study, the effect of a saline flush technique was compared for lesion enhancement, vascular attenuation, and reduction of perivenous artefacts in VMI using

Table 2
The mean value and p value of objective analysis at both 40 keV and the optimal energy; determined as that which achieved the peak contrast-to-noise ratio.

Parameter	40 keV			Optimal keV		
	group A (w/o SF)	group B (w SF)	p-Value	group A (w/o SF)	group B (w SF)	p-Value
Tumour enhancement, HU	193.5±31.1	221.1±32.8	<0.01	98.4±13.9	113.7±15.2	<0.01
Metastatic lymph node enhancement, HU	189.9±41.3	216.4±38.8	0.12	96.2±16.1	109.2±18.2	0.08
Sternocleidomastoid muscle attenuation, HU	105.3±14.0	106.4±13.6	0.52	64.1±7.0	66.2±5.5	0.09
Parotid gland attenuation, HU	89.2±50.6	91.7±63.1	0.71	42.2±26.7	47.7±37.0	0.79
Noise, HU	14.1±2.4	13.3±3.0	0.22	5.3±1.1	5.5±1.1	0.71
Tumour: muscle CNR	6.3±2.3	9±3.1	<0.01	6.6±2.9	9±3.1	<0.01
Metastatic lymph node: muscle CNR	5.8±3.0	8.7±3.8	<0.05	6±4.0	8.1±3.8	0.25
Common carotid artery attenuation, HU						
Injection side	438.4±75.6	428.6±55.0	0.68	198.6±28.2	190.4±53.1	0.46
Opposite side	419.6±64.3	419.5±65.8	0.68	190.9±24.6	186.9±56.1	0.13
Internal juggler vein attenuation, HU						
Injection side	517.3±89.7	461±59.9	<0.01	226.8±34.5	218.5±24.0	0.33
Opposite side	486.7±108.7	462±84.6	0.57	212.9±42.0	219±34.0	0.50
Subclavian vein attenuation, HU						
Injection side	825.9±642.0	466±152.7	<0.01	374.7±333.1	218.9±66.4	<0.05
Opposite side	316±107.9	295.8±74.6	0.59	144±43.9	145.1±33.8	0.71
Superior vena cava attenuation, HU	439.4±137.2	415.2±56.7	<0.05	188.3±57.5	191±26.2	0.53

keV, kilo-electron voltage; w SF, with the saline flush technique; w/o SF, without the saline flush technique; HU, Hounsfield unit; CNR, contrast to noise ratio.

Table 3
The mean value [*k*] and *p*-value of subjective image analysis at both 40 keV and the optimal energy (determined as the enrgy that achieved the peak contrast-to-noise ratio).

Image series		Overall image quality		Delineation of lesion		Perivenous artefact	
0 keV	Group A (w/o SF)	2.70 [0.96]	$p=0.78$	3.04 [0.90]	$p=0.78$	2.44 [0.95]	$p<0.05$
	Group B (w SF)	2.72 [0.96]		3.02 [0.89]		2.74 [0.93]	
Optimal energy	Group A (w/o SF)	3.16 [0.98]	$p<0.05$	2.88 [0.97]	$p=0.59$	3.20 [0.98]	$p<0.05$
	Group B (w SF)	3.40 [0.96]		3.00 [0.98]		3.46 [0.98]	

keV, kilo-electron voltage; w SF, with the saline flush technique; w/o SF, without the saline flush technique; k, kappa value.

fast-kilovoltage switching CT in the head and neck region. In the objective image analysis, the optimal energy was observed at 61 keV for group A and 63 keV for group B. These results are in agreement with those of studies in which lesion CNR was evaluated at differing VMI energy, which reported that optimal CNR was achieved at 60 keV[15] and 65 keV.[13] VMI at 60–65 keV is expected to offer reasonable imaging for tumour detection, planning for radiotherapy, and as a surgical guide in the head and neck region. Indeed, in the present study, the highest score of subjective overall image quality was shown at 61 keV VMI with the saline flush technique. At VMI energy levels ranging from 40 to 80 keV, the CNR of tumours and lymph nodes was higher for group B than group A (Fig 1). This can be explained by the saline flush technique. This technique allowed the efficient use of contrast material by expelling the remaining contrast material in the subclavian vein with saline. Awai *et al.* reported that approximately 20–30 ml of contrast material may remain between the injector and the superior vena cava.[17] As the contrast material volume contributing to tumour imaging increases, tumour attenuation and CNR are enhanced. The difference in optimal

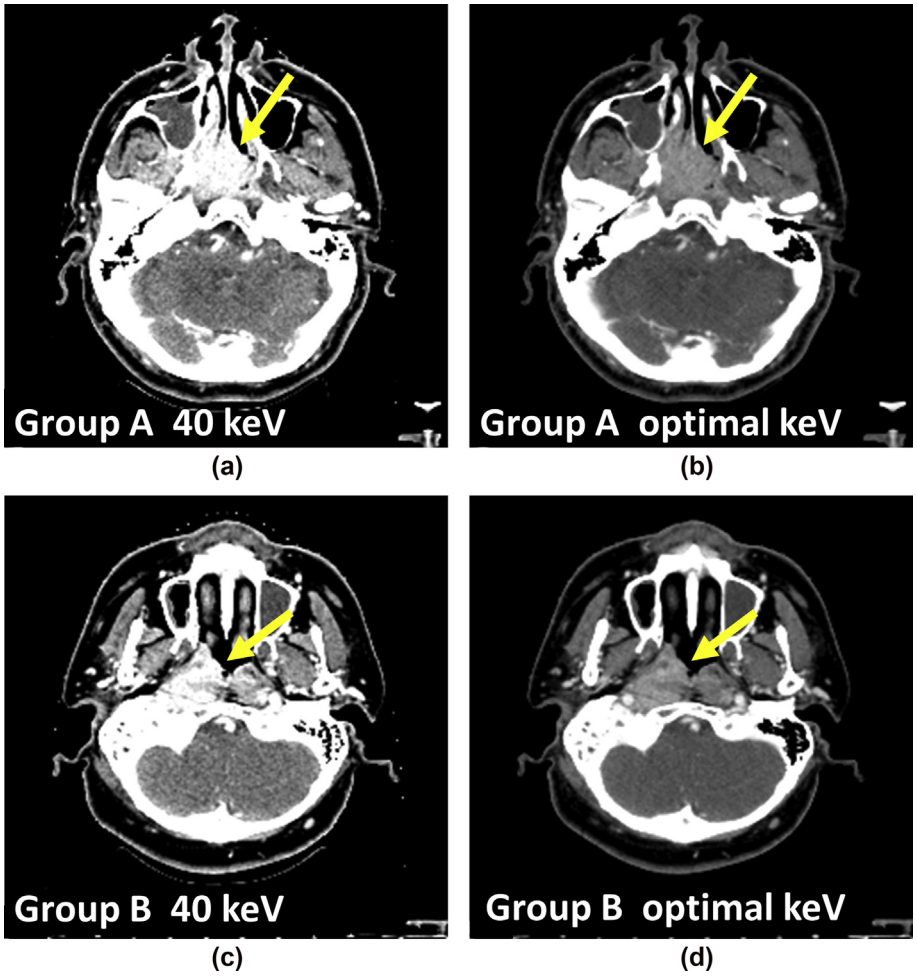

Figure 2 CT images of nasopharyngeal SCC with and without the saline flush technique. Axial CT images of a 65-year-old (a, b) and a 46-year-old patient (c, d) with nasopharyngeal SCC, indicated by arrows. The images of group A (without the saline flush technique at 40 keV (a) and optimal energy (b)) and group B (with the saline flush technique at 40 keV (c) and optimal energy (d)) are shown. Subjective delineation of lesion scores (reviewer 1, 2) were as follows: 2, 2 for (a); 4, 3 for (b); 2, 3 for (c); 4, 4 for (d). Window setting; level 100 HU, width 350 HU.

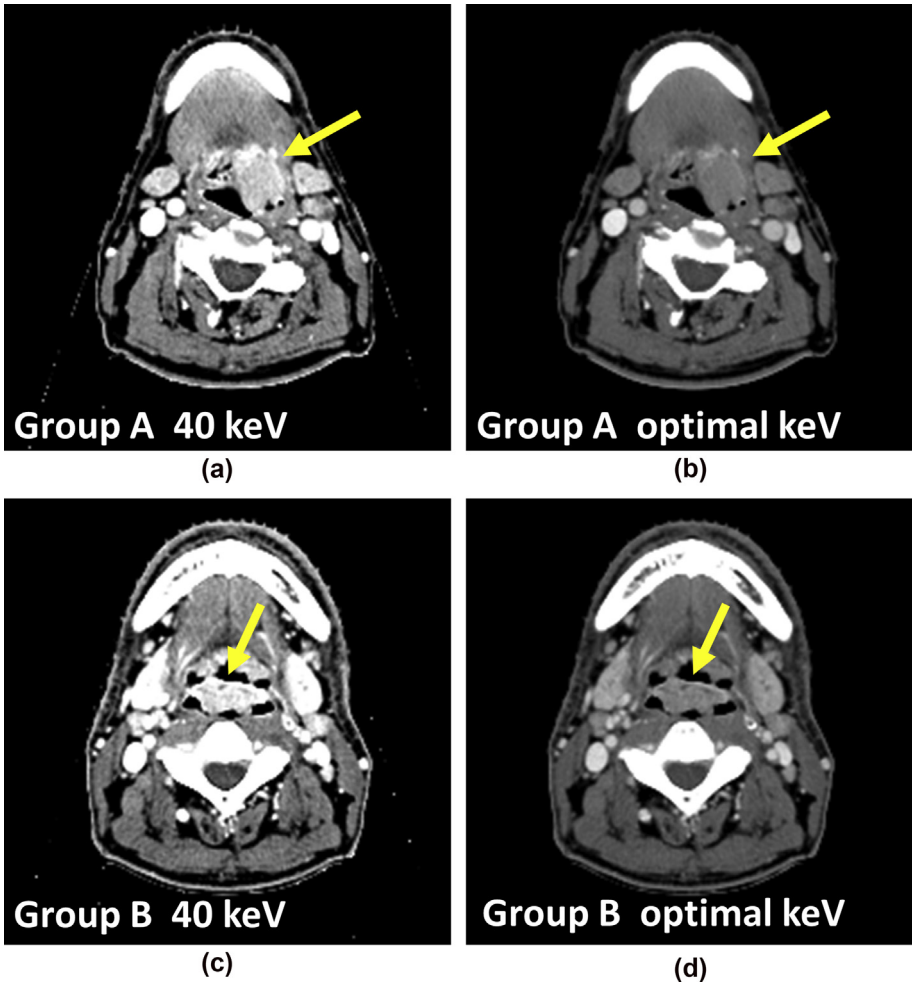

Figure 3 CT images of supraglottic SCC, with and without the saline flush technique. Axial CT images of a 68-year-old (a, b) and a 58-year-old patient (c, d) with supraglottic SCC, indicated by arrows. The images of group A (without the saline flush technique at 40 keV (a) and optimal energy (b)) and group B (with the saline flush technique at 40 keV (c) and optimal energy (d)) are shown. Subjective delineation of lesion scores (reviewer 1, 2) were as follows: 3, 4 for (a); 3, 3 for (b); 2, 4 for (c); 3, 3 for (d). Window setting; level 100 HU, width 350 HU.

energy between groups A and B could be explained in the same way. CNR at a lower energy than the optimal energy gradually declined because the increase in image noise was much higher than the iodine enhancement caused by approaching the k edge. In group B, the increase in iodine enhancement was superior to that in the image noise at lower energy than group A because the amount of contrast material contributing to tumour imaging was much higher than in group A. In addition, the greatest differences in CNR between groups A and B were observed at 40 keV. Thus, the saline flush technique should be used as a standard technique in the head and neck region. In contrast to objective image analysis, which showed significantly higher CNR for group B, significant differences in lesion delineation between both groups were not observed in subjective image analysis. According to the study, which compared image visualisation of head and neck SCC between non-linear image blending and various linear blending in DECT, the tumour CNR seems to correlate with a subjective tumour delineation score.[18] The image that showed the highest tumour CNR also showed the highest subjective tumour delineation score. There are some possible explanations for the discordance. One possibility is a difference in the characteristics of the tumours between both groups. Tumours in head and neck cancer are adjacent to high-density structures (e.g., vertebrae, mandible bone, skull, teeth, and contrast-enhanced salivary glands) and low-density structures (e.g., muscle and fat), hence subjective delineation of tumour score may possibly change depending on the tumour location and size. As shown in Figs 2 and 3, image impressions were different between nasopharyngeal SCC, surrounded by high-density structures, and supraglottic SCC, surrounded by relatively low-density structures. Scholtz *et al.*[18] compared image visualisation using the same patient data between objective groups. The window setting may have affected this discordance. Reviewers were allowed to freely adjust these values in this present study; however, all images were evaluated at specific window setting (level 100 HU; width 350 HU) by both viewers because adjustment of the window setting for 100 individual images takes a lot of time. For tumour delineation, images must be adjusted at a moderate window setting.

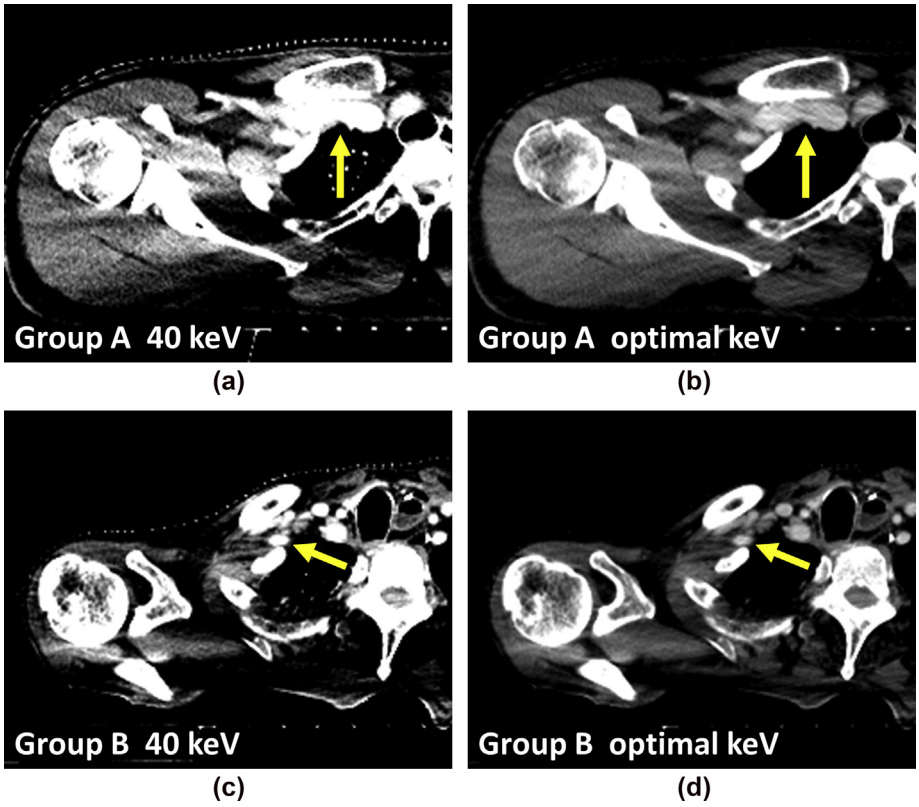

Figure 4 CT images of the costoclavicular space, with and without the saline flush technique. Axial CT images of a 28-year-old (a, b) and a 74-year-old patient (c, d) at the costoclavicular space, indicated by arrows The images group A of (without the saline flush technique at 40 keV (a) and optimal energy (b)) and group B (a with the saline flush technique at 40 keV (c) and optimal energy (d)) are shown. Subjective perivenous artefact scores (reviewer 1, 2) were as follows: 1, 2 for (a); 3, 3 for (b); 3, 4 for (c); 5, 4 for (d). Window setting; level 100 HU, width 350 HU.

It is important to minimise the perivenous artefact for head and neck imaging because the artefact can disturb the depiction of lymph nodes, the subclavian artery, and upper extremity vasculature.[6] Especially, clear depiction of surrounding lymph nodes is essential for radiotherapy contouring. Haage *et al.*[3] has already reported that the perivenous artefact was significantly reduced by using the saline flush technique in conventional CT of the thorax. The first investigation of the saline flush effect at VMI using DECT was conducted in the present study. In accordance with the study reported by Haage *et al.*, the subjective score of perivenous artefact was significantly better for the group with the saline flush technique. As a new insight, the artefact was more prominent at 40 keV VMI than 60–65 keV VMI (Table 3). Although lower energy VMI has the advantage of better tumour depiction than conventional imaging,[2] it has the adverse effect that high attenuation of contrast materials makes perivenous artefacts more prominent. This adverse effect was also shown in the present objective image analysis, which demonstrated higher attenuation of the superior vena cava and injection side venous systems (internal jugular vein and subclavian vein) at 40 keV VMI for the group without the saline flush technique. According to a study that investigated the effect of right or left arm injection on perivenous artefacts, selecting the right arm for contrast material administration could reduce perivenous artefacts without additional cost and effort.[4] Thus, the saline flush technique and selecting the right arm for injection is necessary for the reduction of artefacts, especially when using lower energy VMI.

The present study has several limitations, which should be addressed. Firstly, the volume of saline flush and time delay of scanning for the saline flush protocol is controversial.[6,16,19–21] A volume of 30 ml saline flush and a 10-second time delay of scanning were adopted, according to a previous study, which stated that 30 ml saline flush[21] and a 6-second time delay[16] was a reasonable protocol. Selecting other protocols may result in a different outcome from the present study. Secondly, reviewers were aware that all patients included in this study were suffering from head and neck cancer. This might have influenced the ratings, especially regarding tumour or lymph node delineation, due to greater diagnostic confidence.[15] Finally, direct comparison between using and not using the saline flush technique was not undertaken because patients differed between the two groups. Patient characteristics were not shown to be significantly different between the groups with and without the saline flush in this study; however, it would be desirable for the same patients and tumour locations to be used as study subjects to truly verify the effect of the saline flush effect.

In conclusion, the saline flush technique results in an improvement of tumour and metastatic lymph node CNR and the reduction of perivenous artefact in VMI using DECT. This technique was found to be especially useful at 40 keV

because perivenous artefacts are prominent at lower energy VMI. Subjective overall image quality was found to be highest at 60–65 keV VMI with the saline flush technique.

Conflict of interest

The authors declare no conflict of interest.

Acknowledgements

This study was supported JSPS KAKENHI Grant (Grant-in-Aid for Young Scientists (B) 19K17285).

References

1. May MS, Wiesmueller M, Heiss R, *et al*. Comparison of dual- and single-source dual-energy CT in head and neck imaging. *Eur Radiol* 2018 Oct 18, https://doi.org/10.1007/s00330-018-5762-y.
2. Ginat DT, Mayich M, Daftari-Besheli L, *et al*. Clinical applications of dual-energy CT in head and neck imaging. *Eur Arch Otorhinolaryngol* 2016;**273**:547–53.
3. Haage P, Schmitz-Rode T, Hübner D, *et al*. Reduction of contrast material dose and artefacts by a saline flush using a double power injector in helical CT of the thorax. *AJR Am J Roentgenol* 2000;**174**:1049–53.
4. Yun EJ1, Yoon DY, Han A, *et al*. Central venous stenosis of left versus right arm: its prevalence and effects on image quality in CT of the neck. *Eur J Radiol* 2012;**81**:e126–31.
5. Hopper KD, Mosher TJ, Kasales CJ, *et al*. Thoracic spiral CT: delivery of contrast material pushed with injectable saline solution in a power injector. *Radiology* 1997;**205**:269–71.
6. Takeyama N, Ohgiya Y, Hayashi T, *et al*. Comparison of different volumes of saline flush in the assessment of perivenous artefacts in the subclavian vein during cervical CT angiography. *Br J Radiol* 2011;**84**:427–34.
7. Yamaguchi I, Kidoya E, Suzuki M, *et al*. Evaluation of required saline volume in dynamic contrast-enhanced computed tomography using saline flush technique. *Comput Med Imaging Graph* 2009;**33**:23–8.
8. Kim DJ, Kim TH, Kim SJ, *et al*. Saline flush effect for enhancement of aorta and coronary arteries at multidetector CT coronary angiography. *Radiology* 2008;**246**:110–5.
9. Schoellnast H, Tillich M, Deutschmann HA, *et al*. Improvement of parenchymal and vascular enhancement using saline flush and power injection for multiple-detector-row abdominal CT. *Eur Radiol* 2004;**14**:659–64.
10. Tatsugami F, Matsuki M, Inada Y, *et al*. Usefulness of saline pushing in reduction of contrast material dose in abdominal CT: evaluation of time–density curve for the aorta, portal vein and liver. *Br J Radiol* 2007;**80**:231–4.
11. Matsumoto K, Jinzaki M, Tanami Y, *et al*. Virtual monochromatic spectral imaging with fast kilovoltage switching: improved image quality as compared with that obtained with conventional 120-kVp CT. *Radiology* 2011;**259**:257–62.
12. Große Hokamp N, Laukamp KR, Lennartz S, *et al*. Artefact reduction from dental implants using virtual monoenergetic reconstructions from novel spectral detector CT. *Eur J Radiol* 2018;**104**:136–42.
13. Lam S, Gupta R, Levental M, *et al*. Optimal virtual monochromatic images for evaluation of normal tissues and head and neck cancer using dual-energy CT. *AJNR Am J Neuroradiol* 2015;**36**:1518–24.
14. Wichmann JL, Nöske EM, Kraft J, *et al*. Virtual monoenergetic dual-energy computed tomography: optimization of kiloelectron volt settings in head and neck cancer. *Invest Radiol* 2014;**49**:735–41.
15. Albrecht MH, Scholtz JE, Kraft J, *et al*. Assessment of an advanced monoenergetic reconstruction technique in dual-energy computed tomography of head and neck cancer. *Eur Radiol* 2015;**25**:2493–501.
16. Irie T, Kajitani M, Yamaguchi M, *et al*. Contrast-enhanced CT with saline flush technique using two automated injectors: how much contrast medium does it save? *J Comput Assist Tomogr* 2002;**26**:287–91.
17. Kundel HL, Polansky M. Measurement of observer agreement. *Radiology* 2003;**228**:303–8.
18. Awai K, Hatcho A, Nakayama Y, *et al*. Simulation of aortic peak enhancement on MDCT using a contrast material flow phantom: feasibility study. *AJR Am J Roentgenol* 2006;**186**:379–85.
19. Scholtz JE, Hüsers K, Kaup M, *et al*. Non-linear image blending improves visualization of head and neck primary squamous cell carcinoma compared to linear blending in dual-energy CT. *Clin Radiol* 2015;**70**:168–75.
20. Yoon DY, You SY, Choi CS, *et al*. Multi-detector row CT of the head and neck: comparison of different volumes of contrast material with and without a saline chaser. *Neuroradiology* 2006;**48**:935–42.
21. Behrendt FF, Bruners P, Keil S, *et al*. Effect of different saline chaser volumes and flow rates on intravascular contrast enhancement in CT using a circulation phantom. *Eur J Radiol* 2010;**73**:688–93.